Requirement of Specific Intrahelical Interactions for Stabilizing the Inactive Conformation of Glycoprotein Hormone Receptors*

Angela Schulz‡, Karsten Bruns§, Peter Henklein¶, Gerd Krause‖, Mario Schubert‖, Thomas Gudermann, Victor Wray§, Günter Schultz‡, and Torsten Schöneberg‡ ‡‡**

*From the ‡Institut für Pharmakologie, Universitätsklinikum Benjamin Franklin, Freie Universität Berlin, Thielallee 69–73, 14195 Berlin, Germany, the §Department of Molecular Structure Research, Gesellschaft für Biotechnologische Forschung, Braunschweig, Mascheroder Weg 1, 38124 Braunschweig, Germany, the ¶Institut für Biochemie, Medizinische Fakultät (Charité) der Humboldt-Universität zu Berlin, Schumannstrasse 20/21, 10098 Berlin, Germany, the ‖Institut für Molekulare Pharmakologie, Alfred Kowalke Strasse 4, 10315 Berlin, Germany, and the **Institut für Pharmakologie und Toxikologie, Fachbereich Humanmedizin, Philipps-Universität Marburg, Karl-von-Frisch-Strasse 1, 35033 Marburg, Germany*

Systematic analysis of structural changes induced by activating mutations has been frequently utilized to study activation mechanisms of G-protein-coupled receptors (GPCRs). In the thyrotropin receptor and the lutropin receptor (LHR), a large number of naturally occurring mutations leading to constitutive receptor activation were identified. Saturating mutagenesis studies of a highly conserved Asp in the junction of the third intracellular loop and transmembrane domain 6 suggested a participation of this anionic residue in a salt bridge stabilizing the inactive receptor conformation. However, substitution of all conserved cationic residues at the cytoplasmic receptor surface did not support this hypothesis. Asp/Glu residues are a common motif at the N-terminal ends of α-helices terminating and stabilizing the helical structure (helix capping). Since Asp/Glu residues in the third intracellular loop/transmembrane domain 6 junction are not only preserved in glycoprotein hormone receptors but also in other GPCRs we speculated that this residue probably participates in an N-terminal helix-capping structure. Poly-Ala stretches are known to form and stabilize α-helices. Herein, we show that the function of the highly conserved Asp can be mimicked by poly-Ala substitutions in the LHR and thyrotropin receptor. CD and NMR studies of peptides derived from the juxtamembrane portion of the LHR confirmed the helix extension by the poly-Ala substitution and provided further evidence for an involvement of Asp in a helix-capping structure. Our data implicate that in addition to well established interhelical interactions the inactive conformation of GPCRs is also stabilized by specific intrahelical structures.

G-protein-coupled receptors (GPCRs)[1] comprise a large superfamily of integral membrane proteins that mediate transmembranous signal transduction of a remarkable diversity of ligands (1). Based on the calculated hydrophobicity and their overall structural similarity to bacteriorhodopsin, members of the GPCR superfamily share a predicted structure with seven transmembrane domains (TMD) connected by three alternating extracellular (e1–e3) and intracellular (i1–i3) loops. Low resolution structures deduced from the transmembrane core of rhodopsin, the photoreceptor in retinal rod cells, have confirmed the predicted presence of seven mostly α-helically arranged TMDs (2, 3). However, the current rhodopsin model still lacks detailed structural information of the TMD core and the connecting loops. Several lines of experimental evidence supported a cytosolic α-helical extension of all TMDs (4–12).

As in other polytopic transmembrane proteins, the TMD bundle of GPCRs is primarily arranged to reduce the polar surface area exposed to the hydrophobic membrane environment. Additionally, the functional tertiary structure is formed by establishing specific helix-helix interactions. Site-directed mutagenesis studies with several GPCRs provided compelling evidence for the existence of intramolecular constraining determinants that stabilize an inactive receptor conformation. Mutational alteration of such intramolecular contact sites can lead to constitutive receptor activation. Most of the mutations found to be responsible for constitutive receptor activity are located in the C-terminal portion of the i3 loop (13) and within different TMDs (14). Interhelical salt bridges, as specific structural determinants stabilizing the inactive state, have been identified in rhodopsin (15) and the α_{1B}-adrenergic receptor (16). The identification of such specific contact sites provides most detailed information about the relative orientation of the different helices toward each other.

To date, a large number of activating mutations in the receptors for the glycoprotein hormones thyrotropin (TSHR) and lutropin/choriogonadotropin (LHR) have been identified, providing valuable information on structural requirements of receptor quiescence. Recently, we and others have found an Asp residue within the i3 loop of the TSHR (Asp[619]) and the LHR (Asp[564]) that is necessary to maintain an inactive receptor conformation (17–19). Because the replacement of Asp[564] in the LHR by other amino acid residues except for Glu resulted in agonist-independent receptor activation, it was speculated that agonist- or mutation-induced disruption of a salt bridge involving this conserved Asp residue within the i3 loop contributes to

---

[1] The abbreviations used are: GPCR, G-protein-coupled receptor; hCG, human choriogonadotropin; i3 loop, 3rd intracellular loop; LHR, lutropin/choriogonadotropin receptor; TFE, trifluoroethanol; TSHR, thyrotropin receptor; TMD, transmembrane domain; wt, wild type; PCR, polymerase chain reaction; IP, inositol phosphate.

the active conformation of the glycoprotein hormone receptors.

Herein, we initiated a search for a positively charged amino acid residue in the cytoplasmic portions of the LHR that could potentially provide a counter ion for Asp[564] to form a salt bridge. The identification of such a residue would greatly enhance our knowledge on the spatial arrangement of intracellular receptor loops. Surprisingly, none of the conserved basic amino acids at the cytoplasmic surface participates in a salt bridge with Asp[564]. Specific interaction of the negatively charged side chain of Asp with the peptide backbone often terminates and stabilizes an α-helix at the N-terminal end (N capping) (20, 21). To test for a helix-stabilizing effect of the conserved Asp in the LHR and TSHR, poly-Ala stretches known to form and stabilize α-helices (22–24) were used to replace amino acid residues in the juxtamembrane portion. In functional analyses poly-Ala mutants were not constitutively active even in the absence of the anionic residue. NMR and CD studies with peptides derived from the juxtamembrane portion showed a cytoplasmic extension of TMD6 and provided further indirect evidence of a participation of Asp[564] in a helix-capping structure. Because Asp/Glu residues in the i3 loop/TMD6 junction are conserved in glycoprotein hormone receptors and many other rhodopsin-like GPCRs, we speculate that the inactive receptor conformation depends on the stability of TMD6.

EXPERIMENTAL PROCEDURES

Generation of Mutant LHR and TSHR Genes—All LHR mutations (see Figs. 1 and 2) were introduced into LHR-pcDps (19), a mammalian expression vector containing the entire coding sequence of the human LHR, using a PCR-based site-directed mutagenesis and restriction fragment replacement strategy (25). PCR fragments containing the mutations were digested and used to replace the corresponding *Bsu*36I/*Bst*BI (i1 loop), *Bst*BI/*Xba*I (i2 loop), and *Bst*BI/*Spe*I (i3 loop, C-terminal tail) fragments in the LHR-pcDps. Mutations in the TSHR were generated by exchanging the *Bst*EII/*Bsu*36I fragment within the TSHR-pcDps vector (12) with the corresponding mutant PCR fragment. The identity of the various constructs and the correctness of all PCR-derived sequences were confirmed by restriction analysis and dideoxy sequencing with thermosequenase and dye-labeled terminator chemistry (Amersham Pharmacia Biotech).

Cell Culture, Transfection, and Functional Assays—COS-7 cells were grown in Dulbecco's modified Eagle's medium supplemented with 10% fetal bovine serum, 100 units/ml penicillin, and 100 μg/ml streptomycin at 37 °C in a humidified 7% CO_2 incubator. For transient transfection of COS-7 cells, a calcium phosphate coprecipitation method (26) was applied. Thus, cells were split into 12-well plates (2×10^5 cells/well) and transfected with a total amount of 5 μg of plasmid DNA/well. After 48 h cells were prelabeled with 2 μCi/ml of [³H]adenine (31.7 Ci/mmol; PerkinElmer Life Sciences) and incubated overnight. For cAMP assay, transfected cells were washed once in serum-free Dulbecco's modified Eagle's medium containing 1 mM 3-isobutyl-1-methylxanthine (Sigma), followed by incubation in the presence of the indicated concentrations of human choriogonadotropin (hCG; from pregnancy urine, 3,000 units/ mg, Sigma) or bovine thyrotropin (Sigma); for 1 h at 37 °C. Reactions were terminated by aspiration of the medium and addition of 1 ml of 5% trichloric acid. The cAMP content of cell extracts was determined by anion exchange chromatography as described (27).

To measure inositol phosphate (IP) formation, transfected COS-7 cells were incubated with 2 μCi/ml of myo-³H-inositol (18.6 Ci/mmol; Amersham Pharmacia Biotech) for 18 h. Thereafter, cells were washed once with serum-free Dulbecco's modified Eagle's medium containing 10 mM LiCl. Agonist-induced increases in intracellular IP levels were determined by anion exchange chromatography as described (28).

For radioligand-binding studies, cells were harvested 72 h after transfection (20 μg of plasmid DNA/100-mm dish), and displacement and saturation binding assays were performed using membrane homogenates. Saturation binding studies were carried out for 1 h at 22 °C in a 0.25-ml volume in the presence of 1.2×10^6 cpm of ¹²⁵I-hCG (1800 Ci/mmol; PerklinElmer Life Sciences). Nonspecific binding was defined as binding in the presence of 5 μM hCG. For displacement binding studies, different hCG concentrations were used to displace 100,000 cpm/tube ¹²⁵I-hCG. Purchased ¹²⁵I-hCG was characterized by radioligand receptor assay using the murine LH receptor stably expressed in L cells (29). Saturation binding experiments yielded a K_d value of 0.25

nM for ¹²⁵I-hCG. Data from functional (cAMP assay) and radioligand binding studies were analyzed by a nonlinear curve-fitting procedure using the computer program GraphPad Prism (GraphPad Software, San Diego, CA).

Peptide Synthesis, CD and NMR Spectroscopies, and Structure Calculations—Two peptides i3/TMD6 (NH₂-YATNKDTKIAKKMAILIFTD-FTCMA-CONH₂) and Ala-i3/TMD6 (NH₂-YATNAAAAIAKKMAILIFT-DFTCMA-CONH₂) derived from the amino acid sequence of the LHR i3 loop/TMD6 junction were synthesized by solid phase methodology on a MilliGen 9050 synthesizer using Fmoc (*N*-(9-fluorenyl)methoxycarbonyl) chemistry and TentaGel S RAM resin (Rapp Polymere, Tübingen, Germany). To measure the peptide concentration by spectroscopy at 280 nm, an additional tyrosine was added to the N terminus of both peptides. The crude peptide was purified by reverse-phase high pressure liquid chromatography (30). The correct molecular weights were established by positive ion electrospray mass spectrometry.

CD spectra of peptides i3/TMD6 and Ala-i3/TMD6 were recorded at ambient temperature on a Jasco J-600 spectropolarimeter at a wavelength range from 260 to 180 nm in 0.05-cm cuvettes. The peptides were dissolved at a concentration of 0.2 mg/ml in pure water or in aqueous TFE solutions containing 50% TFE by volume. As these solutions adopted acidic pH value, further measurements were performed in 65 mM phosphate buffer or in phosphate-buffered TFE solution at neutral pH. The resulting curves were smoothed by use of a high frequency filter. Secondary structure content was quantified using the variable selection method (VARSELEC).

For NMR spectroscopy samples of the peptides were dissolved in distilled water (i3/TMD6: 2 mM (5.7 mg/ml), pH 3.0; Ala-i3/TMD6: 0.75 mM (2 mg/ml), pH 3.6) containing 50% TFE-*d₂* by volume to give a final volume of 0.6 ml. ¹H NMR spectra were recorded at 300 K on a Bruker AVANCE DMX 600 instrument using a dedicated 5-mm proton probe head and temperature unit (Haake, Karlsruhe, Germany). The one-dimensional spectra were referenced to sodium 4,4-dimethyl-4-silapentane-1-sulfonate and indirectly to the residual signal of TFE at 3.95 ppm. Two-dimensional phase-sensitive ¹H correlated spectroscopy, total correlation spectroscopy (mixing times of 110 ms), and nuclear Overhauser effect spectroscopy (mixing times of 250 ms) spectra were recorded without spinning and processed using standard Bruker software. For NMR solution spectral assignments a standard procedure was used to establish the unambiguous amino acid spin systems and sequential assignments (31).

The structures were calculated using a simulated annealing protocol and the X-PLOR program, version 3.1 (32, 33). The 222 distance restraints used were categorized with a difference of −0.5 Å as lower bound and with +0.5 Å as upper bound. 1A was added to allow for pseudo atoms. The yielded 20 best energetical structures were superimposed at their α-helical portion and sorted in three different families according their N-terminal tail conformations. The root mean square differences for the backbone atoms and all heavy atoms of a fragment Ala¹-Thr¹⁰ (peptide i3/TMD6) were 0.69 and 1.45 Å, respectively.

Bioinformatics and Molecular Modeling—The protein structure data base Protein Data Bank was searched for proteins encoding a similar potential N-capping sequence motif DTKIAK (LHR i3 loop/TMD6 junction) with the FASTA algorithm of the Genetics Computer Group (Madison, WI) software package. Coordinates of N-capping conformations were used in a three-dimensional structure alignment search algorithm DALI (34) to seek for further Asp containing N-capping helix motifs in the Protein Data Bank data base.

The procedure used to construct the LHR model was described previously for the TSHR (12). Packing of the transmembrane helices was based on electron density maps of frog rhodopsin (3). The LHR structure model was computed with special emphasis on the intracellular portion. The starting conformation of the i1 loop, the i2 loop, and the first portion of the C-terminal tail comprising the putative i4 loop of the LHR were adopted from the NMR structure of the rhodopsin cytosolic loop peptide complex (6) as described for the V2 vasopressin receptor (35). For the starting conformation of the i3 loop and the remaining extracellular loops, fragments of five to eight residues were selected and tested against the Protein Data Bank data base. Fragments occurring more than once with the same backbone conformation in the data base were used for assembling the loops. For the junctional i3 loop/TMD6 fragment, the N-capping conformation identified by FASTA search was employed. All model components were assembled with the biopolymer module of the SYBYL program package (TRIPOS Inc., St. Louis, MO) using the AMBER 4.1 force field (64). Molecular dynamics simulations were performed at 300 K for 200 ps, where only the helix stability was maintained by restraints for hydrogen bonds of the TMD backbones.
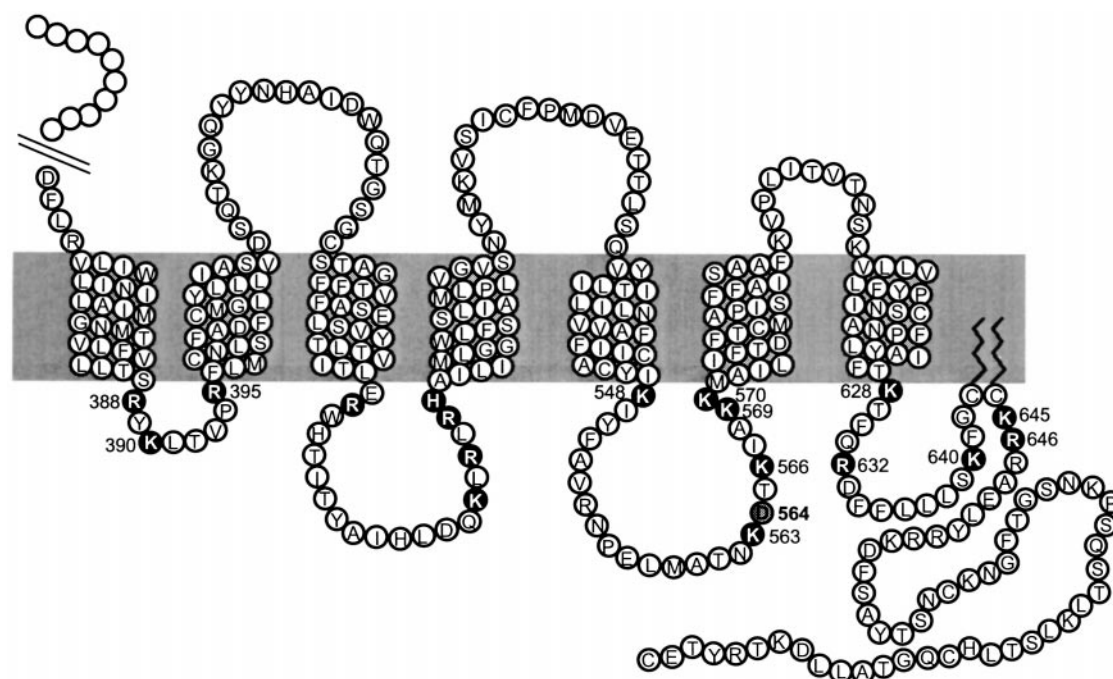
Helix Stability of Glycoprotein Hormone Receptors

FIG. 1. **Localization of conserved basic amino acids within the intracellular loops of the LHR.** The putative arrangement of the LHR within the lipid bilayer is shown. All basic amino acids of the intracellular receptor surface that are conserved among the glycoprotein hormone receptors are shown as *white letters* on a *black background*. To identify a cationic contact site for Asp[564] (*gray background*), all conserved basic amino acids within the intracellular loops (with the exception of Lys[563]; see "Results and Discussion") were replaced by Ala using a site-directed mutagenesis approach.

RESULTS AND DISCUSSION

Screening for a Basic Amino Acid in the Intracellular Loops That Interacts with Asp[564]—We and others have recently identified an anionic amino acid residue (Asp[564]) within the i3 loop of the LHR that is essential for stabilizing the inactive conformation of the receptor (18, 19). The importance of this residue is accentuated further because mutations of the corresponding Asp in the TSHR (Asp[619]) also result in agonist-independent receptor activation (17, 36). Complementary exchange mutagenesis has been successfully used to identify determinants participating in the formation of functionally relevant salt bridges within the transmembrane core of GPCRs (15, 16). In the case of the LHR, identification of the salt bridge-forming counterpart for Asp[564] would provide important information about the fine structure of the cytoplasmatic receptor surface. In a first attempt to identify a positively charged amino acid residue potentially involved in a salt bridge with Asp[564], all conserved basic amino acids in the i2 loop were replaced by Ala residues, and the resulting mutants were tested for constitutive activity (Fig. 1). None of the tested LHR mutants showed constitutively elevated basal cAMP levels in transfected COS-7 cells. All i2 mutants were functionally expressed at the cell surface as illustrated by agonist-dependent cAMP formation (19). Then we extended our study to cationic amino acid residues within the remaining intracellular loops and the cytoplasmic tail that are conserved among mammalian LHR and TSHR. It should be noted that amino acid residues located within portions of the transmembrane helices orientated toward the cytoplasm may also serve as contact partners. However, conserved basic amino acid residues are exclusively distributed within the loops, whereas no basic amino acid residues were found in the TMD region (Fig. 1).

Three cationic residues (Arg[388], Lys[390], and Arg[395]) are preserved in the i1 loop. Functional characterization of Ala substitution mutants (R388A, K390A, and R395A) revealed no constitutive activity. All three mutant LHR displayed decreased hCG-induced E_{max} values probably because of a 12–76% reduction in cell surface expression (Table I). Basal receptor activity depends on its cell surface expression, and one can argue that constitutive activity of a mutant receptor is masked by intracellular receptor retention. However, elevated basal activity of mutant LHR can be monitored even if the cell surface expression is reduced to 12% of the wild type (wt) LHR (19, 37).

In the i3 loop five basic amino acid residues (Lys[548], Lys[563], Lys[566], Lys[569], and Lys[570]) are conserved in the mammalian LHR and TSHR (Fig. 1). Arg[554] in the human LHR is replaced by Gln in the bovine, pig, rat, mouse, and sheep LHR and was therefore not taken into consideration. Because Lys[563] has been previously deleted in the human LHR without affecting the basal and agonist-induced cAMP formation (19), participation of this residue in a salt bridge with the adjacent residue Asp[564] appears unlikely. Ala substitution of the remaining Lys residues had no effect on basal receptor activity (Table I). The efficacy of hCG-induced cAMP accumulation was comparable with the wt LHR. Only K570A showed a reduced E_{max} value as the result of a lower cell surface expression. The latter finding is in good agreement with studies on the human TSHR showing that mutation of the corresponding position (R625) does not induce constitutive activity and decreases the TSHR plasma membrane expression (38). The *BXXBB* motif (where *B* indicates a basic amino acid and *X* indicates any amino acid) at the i3 loop/TMD6 junction is highly conserved within glycoprotein hormone receptors, and it was suggested that this motif can form a functionally relevant amphiphilic helix. In agreement with our studies, simultaneous substitution of all three cationic residues with Ala had no functional consequence as compared with the wt rat LHR (39).

Finally, we successively mutated all conserved basic residues (Lys[628], Arg[632], Lys[640], Lys[645], and Arg[646]) in the cytoplasmic receptor tail. All Ala substitutions did not significantly influence basal receptor activity and agonist-induced cAMP forma-

TABLE I
Functional characterization of LHR Ala mutants

COS-7 cells were transfected with various LHR mutants. Functional assays were carried out as described under "Experimental Procedures." cAMP levels are expressed as fold of wt LHR basal levels (193 ± 44 cpm/well). In IP accumulation assays, basal IP levels were similar for wt and all mutant LHRs (399 ± 159 cpm/well). Increases in cAMP and IP levels were obtained from stimulation with 100 and 500 nM hCG, respectively. B_{max} values were determined by saturation binding experiments (see "Experimental Procedures"). Binding studies with the wild type LHR (LHR(wt)) revealed a B_{max} value of 8,000–13,000 receptors/cell, and receptor densities of the mutant LHR are expressed as percentages of expression of the LHR(wt). Data are presented as the means ± S.E. of two to four independent experiments, each carried out in duplicate (binding assay) or triplicate (cAMP and IP assays).

Transfected construct	^{125}I-hCG binding (B_{max})	cAMP assays		IP assays (increase in IP levels)
		Basal cAMP levels	Increase in cAMP levels	
	% LHR(wt)	*fold above wt basal*		*fold above basal*
LHR(wt)	100	1.0	7.6 ± 3.7	3.2 ± 0.8
R388A	88.3 ± 10.3	1.2 ± 0.1	4.9 ± 0.9	2.0 ± 0.5
K390A	63.3 ± 22.4	1.0 ± 0.1	3.1 ± 0.6	1.9 ± 0.5
R395A	24.1 ± 9.1	0.9 ± 0.1	5.6 ± 4.4	1.6 ± 0.7
K548A	62.4 ± 8.7	1.1 ± 0.1	10.8 ± 6.5	2.1 ± 0.8
K566A	89.3 ± 19.6	0.9 ± 0.1	7.8 ± 5.2	2.4 ± 0.7
K569A	72.1 ± 33.2	1.0 ± 0.1	10.5 ± 6.2	2.4 ± 0.7
K570A	31.9 ± 14.6	0.9 ± 0.1	4.9 ± 2.8	1.6 ± 0.7
K628A	43.2 ± 15.3	1.1 ± 0.2	4.8 ± 2.7	2.0 ± 0.8
R632A	31.9 ± 15.9	1.0 ± 0.2	8.8 ± 4.9	2.0 ± 0.6
K640A	66.2 ± 2.9	0.9 ± 0.2	5.8 ± 3.3	1.7 ± 0.6
K645A	57.2 ± 17.9	0.9 ± 0.1	8.6 ± 4.1	2.3 ± 0.5
R646A	63.5 ± 5.5	0.9 ± 0.1	7.3 ± 1.6	2.3 ± 0.6

tion (Table I). These results were in congruence with previous mutagenesis studies in the C-terminal region. Truncation mutants of the cytoplasmic tail of the rat LHR at position 631 and mouse LHR at the position 628 (corresponding position 627 in the human LHR) that include all conserved basic amino acids in the C-terminal tail showed a reasonable agonist-induced cAMP formation but did not display agonist-independent activity (40, 41).

Additionally, all Ala substitution mutants were analyzed in an IP accumulation assay. Stimulation of wt LHR expressing cells with 500 nM hCG resulted in a 3-fold increase in IP levels (Table I). Most of the Ala LHR mutants that were expressed at considerably lower receptor densities than the wt LHR showed a reduced efficacy in response to agonist challenge. It should be noted that none of the mutant LHRs showed constitutive activity toward the IP signaling pathway.

Utilizing an Ala substitution approach, a potential interaction partner that participates in a salt bridge with Asp[564] was not identified. Interestingly, none of the 17 Ala substitution mutants displayed a complete loss-of-function despite the fact that the orientation of membrane proteins is determined by the asymmetric distribution of charged residues in the sequences flanking the transmembrane domains. The net charges of the amino acid residues flanking the transmembrane region of the LHR are in good agreement with the "positive inside rule." Numerous studies have shown that an excess of positively charged residues defines a cytoplasmic domain of a membrane protein and, therefore, determines the orientation and topology of the transmembrane segments (42).

Rescue of LHR and TSHR wt Function by Poly-Ala Substitutions—Because our mutagenesis data gave no further support for a salt bridge, other possible functions of Asp[564] were taken into consideration. The N- and C-terminal ends of TMDs are usually predicted by hydrophobicity analysis (43). There is compelling experimental evidence that the helical character of the TMDs continues into the loops (see the Introduction). At one point the helix must be terminated to allow for a loop turn. Because of a lower number of intrahelical interactions, an α-helix becomes more flexible at both ends. Several so called capping motifs have been identified at the very N- and C-terminal ends of helices, terminating and stabilizing the downstream and upstream helix, respectively (21, 44, 45). Recently, an extensive sequence/structure analysis demonstrated that

the Asp side chain carboxylate forms a hydrogen bond with the i+2 or i+3 NH moiety of the peptide backbone as a common feature of the N termini of α-helices. Such hydrogen bonds within an N cap structure can also be formed by the side chain amide group of Asn (21). However, Asn is not always equivalent to Asp in maintaining a stable N cap structure. The additional stabilization afforded by Asp relative to Asn either may be due to stronger H bonding via a negatively charged oxygen *versus* the neutral oxygen of Asn or by a favorable interaction between the negatively charged side chain and the helix macrodipole (46). Such a mechanism probably reflects the situation in the LHR in which Asp[564] substitution by Asn results in a lower constitutive activation of the receptor as compared with other Asp[564] mutants (18, 19). We therefore speculated that Asp[564] participates in TMD6 stabilization by formation of an N cap structure. A common sequence motif in an N-terminal capping box is (S/T)*XX*(E/D) (20, 47, 48). This motif is present in the human LHR (position 561–564 in Fig. 1), but the functional relevance of the threonine in stabilizing the TMD6 is questioned because serine or threonine residues at the indicated position are not preserved among glycoprotein hormone receptors, *e.g.* human TSHR. Additionally, substitution of Thr[561] in the human LHR by glycine (LHR T561G) did not result in an elevation of the basal LHR activity.[2]

It is well established that because of the hydrophobicity and the lack of disturbing side chain interactions, poly-Ala based peptides easily adopt a stable α-helical structure in different environments. Therefore, poly-Ala stretches were successfully used to achieve helix stabilization and even rescue helical structures in peptides and soluble proteins (22, 24, 49). We hypothesized that introduction of poly-Ala stretches at the i3 loop/TMD6 junction of the LHR can mimic the structural function of an N-capping motif by extending TMD6 more into the cytosol and, therefore, stabilizing the helical character of the downstream polypeptide chain. To address our hypothesis experimentally, we generated a mutant LHR in which amino acid residues 558–566 were replaced by Ala (LHR-558–566A; Fig. 2*A*). As predicted, functional characterization of this poly-Ala substitution mutant in COS-7 cells revealed no basal constitutive activity even in the absence of a negatively charged amino

---

[2] A. Schulz and T. Schöneberg, unpublished data
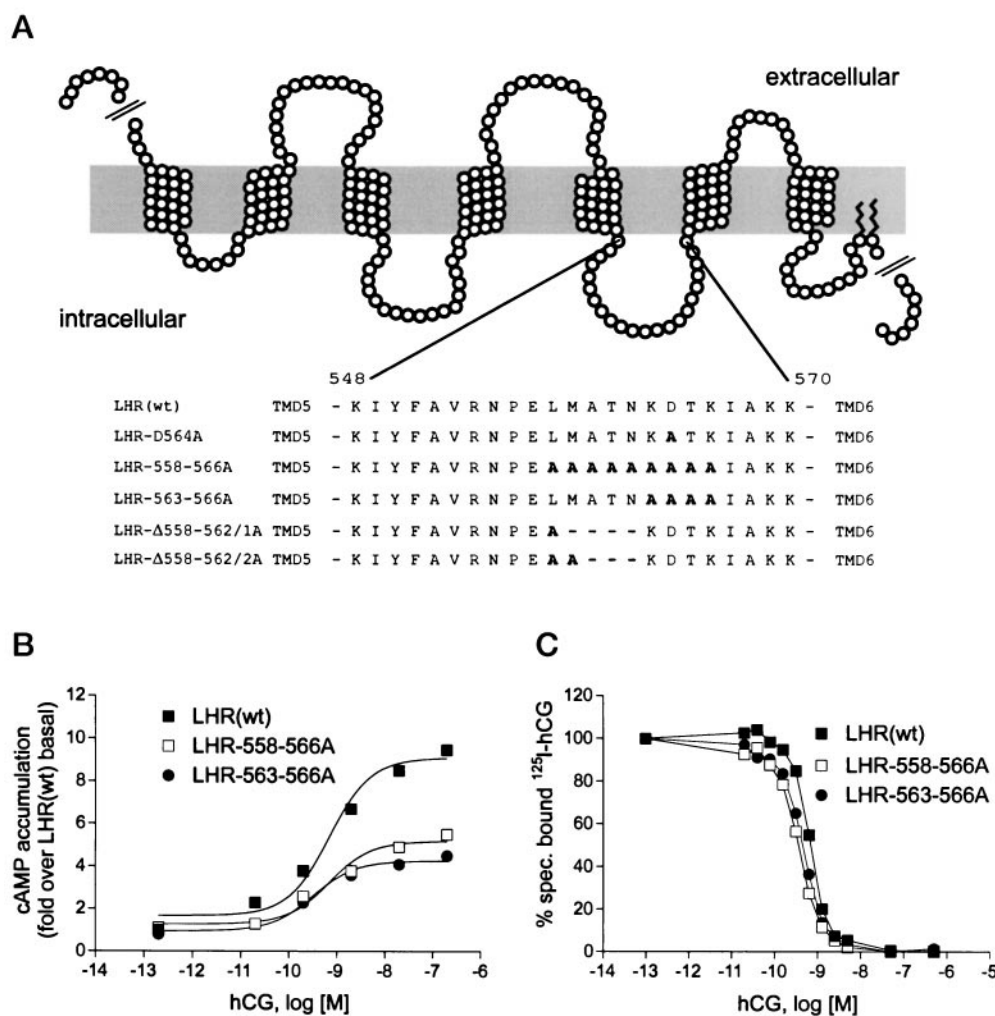
FIG. 2. **Functional analysis of poly-Ala substitutions within the i3 loop of the LHR.** To study the functional consequence of multiple Ala substitutions within the i3 loop, five mutant LHR were generated (*A*). The various LHR mutants were expressed in COS-7 cells, and cAMP accumulation assays (*B*) and ^{125}I-hCG displacement studies (*C*) were performed as described under "Experimental Procedures." Data are presented as means of three independent experiments, each carried out in duplicate. See also Table II.

acid residue at position 564 (Table II). The cell surface expression and maximal hCG-induced cAMP formation were reduced by approximately 40% compared with the wt LHR. Next, we asked whether the length of the Ala substitution can be reduced without generating a constitutively active LHR. Thus, a four-Ala substitution mutant including Asp^{564} (LHR-563–566A) was tested in cAMP accumulation assays. Consistently, the LHR-563–566A displayed wt LHR function. To examine agonist potency and binding properties at the wt LHR and mutant receptors, both Ala substitution mutants were studied in concentration-response experiments and in radioligand displacement assays. As shown in Fig. 2 (*B* and *C*), no significant differences in the EC_{50} and K_i values were observed when compared with the wt LHR (Table II). In congruence with previous studies (18) single Ala substitution of Asp^{564}, however, resulted in a constitutively active receptor (Table II). Basal and hCG-induced IP accumulation remained unchanged in all Ala mutants as compared with the wt receptor (Table II).

To investigate whether helix stabilization by poly-Ala stretches is a general phenomenon and also applies to other glycoprotein hormone receptors, we studied the functional consequence of a four-Ala substitution at the corresponding positions 618–621 in the TSHR (TSHR-618–621A). We demonstrated that similar to the LHR, the N-terminal extension of TMD6 in the TSHR-618–621A did not interfere with proper

receptor function as determined by the potency and efficacy of the thyrotropin-induced cAMP formation (Table II).

Taken together, these results strongly suggest a helix-stabilizing effect of Asp^{564} and Asp^{619} in the LHR and the TSHR, respectively, and support the observation that a salt bridge including these residues within both glycoprotein hormone receptors is not involved in maintaining the inactive receptor conformation. Because wt receptor function can be mimicked by short hydrophobic stretches of Ala, our data are indicative of a local effect on TMD6 stability and also exclude the possibility of a salt bridge with an unidentified signal transduction component downstream of the receptor.

Direct Structural Evidence for N-terminal Helix Extension by Poly-Ala Substitution—Currently, a high resolution structure for any GPCR is not available because of the difficulties inherent in producing, purifying, and crystallizing integral membrane proteins. Based on the experimental evidence above that Asp^{564} participates in an N cap structure and poly-Ala substitutions imitate the function of Asp^{564}, we attempted to directly answer three questions by CD and NMR spectroscopies of peptides derived from the i3 loop/TMD6 junction. First, we asked whether TMD6 of the LHR is extended into the cytosol as found for other GPCRs. Second, is Asp^{564} included in the helical portion or located in a proper proximity to the N terminus of TMD6 to ensure an N cap formation? It should be noted that

TABLE II

Functional consequence of poly-Ala substitution in the i3 loop of the LHR and the TSHR

Following COS-7 cell transfection with LHR and TSHR mutants, functional assays were carried out as described under "Experimental Procedures." Basal and hCG-induced (100 nM) cAMP levels are expressed as fold of LHR(wt) basal levels (193 $\pm$ 44 cpm/well). EC$_{50}$ values were determined by performing cAMP assays with increasing concentrations of hCG (10 pM to 100 nM hCG). The TSH-induced cAMP accumulation (100 milliunits bovine thyrotropin/ml) is expressed as fold over wt TSHR basal cAMP levels (375 $\pm$ 90 cpm/well). In IP accumulation assays, no differences in basal IP levels were found for all mutant LHRs (238 $\pm$ 70 cpm/well), and hCG-induced (500 nM) IP levels were expressed as increases above basal IP levels. B$_{max}$ values were determined by saturation binding experiments (see "Experimental Procedures"). ^{125}I-hCG displacement studies were performed for K_i value determination of the individual mutant LHR. Data are presented as the means $\pm$ S.E. of two to four independent experiments, each carried out in duplicate (binding assay) or triplicate (cAMP and IP assays).

Transfected construct	^{125}I-hCG binding		cAMP assays			IP assay (increase in IP levels)
	B$_{max}$	K_i	Basal cAMP levels	Increase in cAMP levels	EC$_{50}$	
	% LHR(wt)	*nM*	*fold of wt basal*	*fold of wt basal*	*nM*	*fold of basal*
LHR(wt)	100	0.66	1.0	7.1 $\pm$ 1.7	0.25	3.2 $\pm$ 0.9
LHR-D564A	[a]	[a]	1.8 $\pm$ 0.6	9.6 $\pm$ 5.1	[a]	1.8 $\pm$ 0.1
LHR-558–566A	57.6 $\pm$ 6.4	0.35	1.1 $\pm$ 0.2	5.2 $\pm$ 1.2	0.22	3.3 $\pm$ 0.9
LHR-563–566A	68.0 $\pm$ 3.0	0.44	0.8 $\pm$ 0.3	6.8 $\pm$ 1.5	0.27	3.7 $\pm$ 1.0
LHR-Δ558–562/1A	81.1 $\pm$ 29.2	[a]	1.1 $\pm$ 0.2	4.7 $\pm$ 1.4	0.18	3.4 $\pm$ 0.9
LHR-Δ558–562/2A	202 $\pm$ 12.7	[a]	0.9 $\pm$ 0.2	8.1 $\pm$ 2.8	0.13	3.4 $\pm$ 1.1
TSHR(wt)	[a]	[a]	1.0	4.3 $\pm$ 0.2	0.58[b]	[a]
TSHR-618–621A	[a]	[a]	0.8 $\pm$ 0.1	4.3 $\pm$ 1.4	0.55[b]	[a]

[a] Not determined.
[b] Values indicated are measured in milliunits/ml.

the spectroscopic methods used are unable to directly demonstrate a helix-capping structure. Additionally, it has to be taken in consideration that peptides derived from the i3 loop/TMD6 junction showed intrinsic activity in stimulating the G$_s$ protein (50, 51), and the i3/TMD6 peptide in the chosen environment (solvent, pH value) may already adopt the active conformation. Third, does a poly-Ala substitution indeed extend the N terminus of TMD6? The third question arises from reports that poly-Ala stretches not necessarily form α-helices (52). Thus, a peptide (i3/TMD6) derived from the sequence of the i3 loop/TMD6 junction of the LHR (amino acid position 560–583) was synthesized and analyzed by CD and NMR spectroscopies. The data were compared with those from a peptide (Ala-i3/TMD6) in which the amino acid residues 563–566 were replaced by four Ala.

Initially, CD analysis was performed to obtain general information about the structure and folding of both peptides. In aqueous solution (pH 4.0), the initial shallow negative CD curve of the wt LHR-derived peptide (i3/TMD6) was characteristic of a disordered peptide conformation with very little evidence of stable secondary structure (Fig. 3A). Adjusting the pH value to 7.2, the CD spectrum of the peptide i3/TMD6 displayed a positive band at 190 nm and a shift of the negative ellipticity to ~220 nm, which is indicative of a significant portion of helical structure. As shown in Fig. 3B the peptide Ala-i3/TMD6 already possessed curves at pH 4.2 similar to those found for i3/TMD6 at pH 7.2. Next, the effect of an organic solvent (50% TFE) that mimics the hydrophobic transmembrane environment more closely was tested. A substantial negative ellipticity developed at ~220 nm and a positive band at 190 nm that were indicative of an increasing content of stable helical secondary structure. Estimation of the helical content by standard methods (53) revealed ~55.2% and 61.6% helical structure for i3/TMD6 and Ala-i3/TMD6, respectively, at a pH value of 4.2. Increase of the pH value (pH 7.2) led to a reduction in helical content in both peptides with 44.6% for i3/TMD6 and 39.2% for Ala-i3/TMD6 probably because of aggregation (see below). In solution, hydrophobic membrane-spanning peptides such as i3/TMD6 tend to be insoluble or tend to aggregate. Such aggregates are frequently composed of unfolded forms of the peptide or multimeric β-sheet-like structures in which the secondary structure does not represent the native fold (54–56). In an initial step we therefore focused on the production of a monomeric form of the peptides suitable for NMR measurements. As
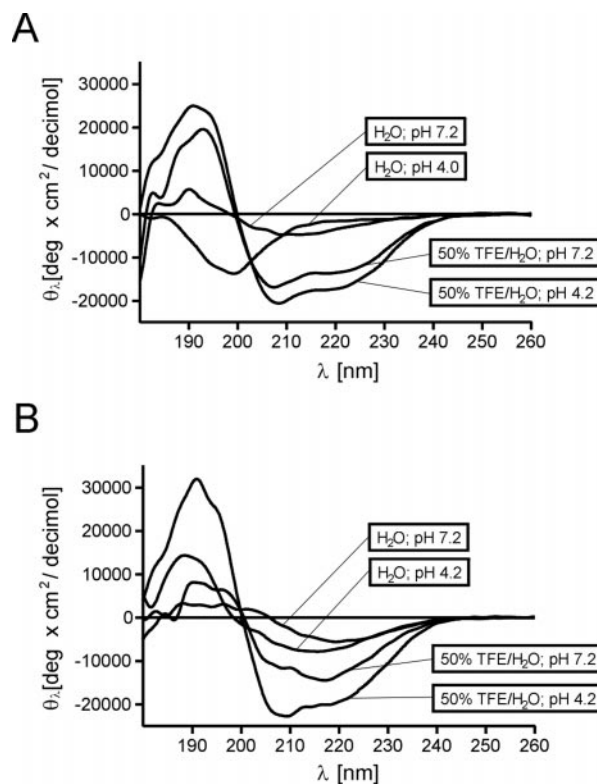

FIG. 3. **CD spectra of the peptides representing the i3 loop/TMD6 junction of the wt LHR and the LHR-563–566A.** CD data of the peptide i3/TMD6 (*A*) and the peptide Ala-i3/TMD6 (*B*) (both 0.2 mg/ml) were obtained in water and in the presence of 50% TFE/water (v/v) at different pH values.

expected from the CD analysis, initial high resolution NMR data in aqueous solution were characterized by linewidths preventing structural analysis (data not shown). It has been demonstrated for peptides derived from GPCRs and other transmembrane proteins that lipomimetic solvents such as TFE contributes to the stability of α-helical TMDs (57, 58), but the overall structural adoption of the peptides did not present major differences as compared with NMR studies using micelles for peptide solubilization (8, 59). As a result of these initial NMR studies, all subsequent NMR experiments were
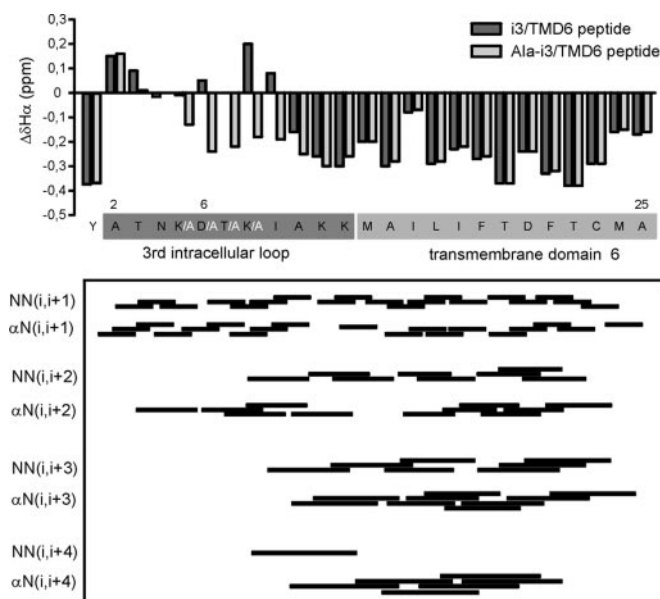
FIG. 4. **Structural analyses of the peptides i3/TMD6 and Ala-i3/TMD6 by NMR spectroscopy.** Two peptides, i3/TMD6 and Ala-i3/TMD6, derived from the amino acid sequence of the LHR i3 loop/TMD6 junction were analyzed by NMR spectroscopy. Asp at position 6 corresponds to Asp[564] in the LHR sequence. α-Proton chemical shift differences ($\Delta\delta H\alpha = \delta H\alpha_{observed} - \delta H\alpha_{random\ coil}$) for both peptides, i3/TMD6 and Ala-i3/TMD6, dissolved in 50% TFE/water (v/v) at pH 3.0 and 3.6 are presented as parts per million (*upper panel*). A summary of short range and medium range NOE signals of the peptide i3/TMD6 is shown in the *lower panel*.

performed in 50% aqueous TFE at lower pH values (3.0 to 3.6) because peptides tend to aggregate at higher pH values, thus preventing further assessments.

The through-bond connectivities of the various amino acid spin systems were identified from two-dimensional ¹H phase-sensitive correlated spectroscopy and total correlation spectroscopy spectra starting from the amide protons in the region 8.9–7.5 ppm and were confirmed by inspection of cross-peaks in the high field region corresponding to side chain connectivities. The Hα chemical shifts are strongly dependent on the nature of protein secondary structure in both proteins and peptides. Hence, helices are present when four adjacent residues show upfield shifts greater than 0.1 ppm, whereas downfield shifts of three adjacent residues greater than 0.1 ppm are indicative of a β-strand (60). Fig. 4 (*upper panel*) shows the situation found for both peptides. According to the above criterion, there is strong evidence that the i3/TMD6 peptide forms an α-helix in the region between Ala[10] and Ala[25]. Substitution of the amino acid residues 5–8 by Ala resulted in an N-terminal extension of the α-helix now encompassing the region Ala[5]–Ala[25]. These results are in good agreement with the hypothetical structural consequence resulting from a poly-Ala substitution in the i3 loop of the LHR. To further support the presence of an α-helix, the secondary structure in the i3/TMD6 peptide was determined from the identification of a large number of short range and medium range connectivities, which are well distributed over the entire sequence (Fig. 4, *lower panel*). Contiguous stretches of HN-HN(i, i+3), Hα-HN(i, i+3), and Hα-HN(i, i+4) nuclear Overhauser effect signals are indicative for an α-helical structure comprising amino acid residues 10–25. Moreover, structure calculations of the peptide i3/TMD6 based on 222 NMR-NOE distance restraints clearly confirmed an α-helix structure corresponding to the region Ala[10]–Ala[25] (Fig. 5). NMR data suggest an N-terminal extension of TMD6 beyond the transmembrane portion as shown for rhodopsin and the β-adrenoreceptor (6, 7, 9, 11). Although transmembrane
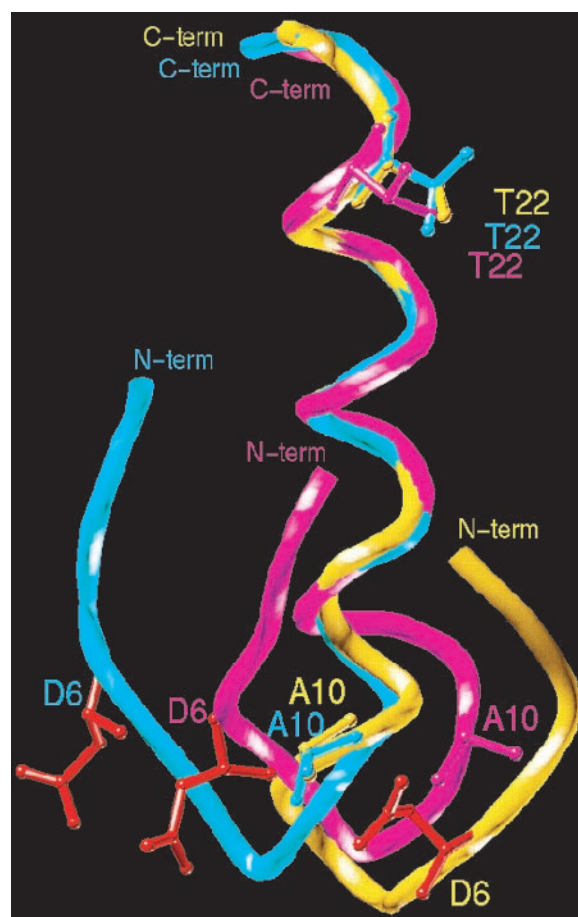

FIG. 5. **Structure models of the peptide i3/TMD6 from simulated annealing and refinement calculations.** Superposition of the 20 best final restrained structures of the peptide i3/TMD6 in 50% TFE were summarized in three major groups after alignment (*blue*, *magenta*, and *yellow*) of the backbone atoms Met[13]–Ala[25]. Residue numbering has been included for each structural family to facilitate the recognition of the regions. Asp at position 6 (*red side chain*) corresponds to Asp[564] in the LHR sequence. *N-term*, N terminus; *C-term*, C terminus.

predictive methods provide Met[571] (Met[13] in the peptides) as the TMD-terminating residue, it is interesting that residues Ala[10]–Lys[12] are α-helical in a lipomimetic medium. Based on TMD predictions, this region would lie to the cytosolic side of the membrane. The two sequential lysine residues at positions 569 and 570 are consistent with the positive inside rule for type I transmembrane sequences acting as a stop transfer signal for membrane insertion (61). In contrast, the N-terminal parts but not the C terminus of both peptides lacked defined structures within the limits of detection because of minor inter-residue structure constraints that allow more flexibility. Superposition of the 20 best energetical structures of the peptide i3/TMD6 revealed three different families of conformations with an almost identical α-helical portion but differences in their N-terminal tail conformations (Fig. 5). In the peptide i3/TMD6, Asp[6], which corresponds to Asp[564] in the wt LHR receptor, is located within the flexible portion. In principle, the close proximity of Asp[6] to the N terminus of the α-helical part (Ala[10]) enables the Asp side chain to participate in an N-terminal helix-capping structure. Taken together, CD and NMR studies with peptides derived from the i3 loop/TMD6 junction provided direct evidence that an N-terminal extension and probably stabilization of TMD6 is the structural consequence of mutationally introduced poly-Ala stretches that have been shown to mimic the stabilizing function of Asp[564] at the N-terminal end of TMD6.

TABLE III
Amino acid sequence alignment of the i3 loop/TMD6 junction of selected family 1 GPCRs

Amino acid sequences of members of the rhodopsin-like GPCR family were taken from the GPCR data base (GPCRdb at EMBL, Heidelberg), and sequences of the i3 loop/TMD6 junction were aligned. The conserved Asp/Glu residues corresponding to Asp[564] in the LHR (*) and the highly conserved proline in TMD6 (#) are indicated. The receptors are sorted by ligands and named in regard to their citation in the GPCR database.

| Family 1 GPCRs	Name	Sequence
		* #
Glycoprotein hormone receptors	LSHR_HUMAN	DTKIAKKMAILIFTDFTCMAP
	FSHR_HUMAN	DTRIAKRMAMLIFTDFLCMAP
	TSHR_HUMAN	DTKIAKRMAVLIFTDFICMAP
Opsins	OPSB_HUMAN	EREVSRMVVVMVGSFCVCYVP
	OPSD_HUMAN	EKEVTRMVIIMVIAFLICWVP
	OPSG_HUMAN	EKEVTRMVVVMVLAFCFCWGP
	OPSR_HUMAN	EKEVTRMVVVMIFAYCVCWGP
Adrenergic receptors	A1AA_HUMAN	EKKAAKTLGIVVGCFVLCWLP
	A2AA_HUMAN	EKRFTFVLAVVIGVFVVCWFP
	B1AR_HUMAN	EQKALKTLGIIMGVFTLCWLP
	B2AR_HUMAN	EHKALKTLGIIMGTFTLCWLP
	B3AR_HUMAN	EHRALCTLGLIMGTFTLCWLP
Dopamine receptors	DADR_HUMAN	ETKVLKTLSVIMGVFVCCWLP
	D2DR_HUMAN	EKKATQMLAIVLGVFIICWLP
	D3DR_HUMAN	EKKATQMVAIVLGAFIVCWLP
	D4DR_HUMAN	ERKAMRVLPVVVGAFLLCWTP
Serotonin receptors	5H1A_HUMAN	ERKTVKTLGIIMGTFILCWLP
	5H2A_HUMAN	EQKACKVLGIVFFLFVVMWCP
	5H5A_HUMAN	EQRAALMVGILIGVFVLCWIP
	5H7_HUMAN	EQKAATTLGIIVGAFTVCWLP
Histamine receptors	HH1R_HUMAN	ERKAAKQLGFIMAAFILCWIP
	HH2R_HUMAN	EHKATVTLAAVMGAFIICWFP
Muscarinic acethylcholine receptors	ACM1_HUMAN	EKKAARTLSAILLAFILTWTP
	ACM2_HUMAN	EKKVTRTILAILLAFIITWAP
	ACM3_HUMAN	EKKAAQTLSAILLAFIITWTP
	ACM4_HUMAN	ERKVTRTIFAILLAFILTWTP
Adenosine receptors	AA1R_HUMAN	ELKIAKSLALILFLFALSWLP
	AA2A_HUMAN	EVHAAKSLAIIVGLFALCWLP
	AA3R_HUMAN	EFKTAKSLFLVLFLFALSWLP
Somatostatin receptors	SSR1_HUMAN	ERKITLMVMMVVMVFVICWMP
	SSR2_HUMAN	EKKVTRMVSIVVAVFIFCWLP
	SSR3_HUMAN	ERRVTRMVVAVVALFVLCWMP
	SSR5_HUMAN	ERKVTRMVLVVVLVFAGCWLP
Bradykinin receptors	BRB1_HUMAN	DSKTTALILTLVVAFLVCWAP
	BRB2_HUMAN	ERRATVLVLVVLLLFIICWLP
Melatonin receptors	ML1A_HUMAN	DFRNFVTMFVVFVLFAICWAP
	ML1X_HUMAN	EVRNFLTMFVIFLLFAVCWCP
Cannabinoid receptors	CB1R_HUMAN	DIRLAKTLVLILVVLIICWGP
	CB2R_HUMAN	DVRLAKTLGLVLAVLLICWFP
Prostaglandin receptors	PE21_HUMAN	DVEMVGQLVGIMVVSCICWSP
	PD2R_HUMAN	ELDHLLLLALMTVLFTMCSLP
	TA2R_HUMAN	EVEMMAQLLGIMVVASVCWLP
Orphan GPCR	GPRL_HUMAN	DKRYAMVLFRITSVFYILWLP
Olfactory	OLF2_HUMAN	EDTSYNEIQVAVASVFILVVP

α-Helix Stability, a Possible Molecular Switch for Receptor Activation—To further support the idea of an involvement of Asp[564] in a helix-stabilizing structure, we searched for the presence of Asp/Glu residues corresponding to the position of Asp[564] in other members of rhodopsin-like GPCRs. As shown in Table III Asp/Glu residues at the N-terminal end of TMD6 are a common sequence motif in a large number of GPCRs including rhodopsin, receptors for amines, peptides, and lipids. Asp (58 hits) or Glu (345 hits) residues 20 amino acids upstream of a highly conserved Pro in TMD6 were found in 403 (37%) out of 1099 rhodopsin-like GPCRs (GPCR data base, GPCRdb, EMBL, Heidelberg). The presence of Asp/Glu residues was independent of their G-protein-coupling preference (*e.g.* adrenergic receptors). It should be noted that our sequence analysis probably underestimates the number of Asp/Glu residues as possible candidates for an N cap of TMD6. Several GPCRs contain an anionic residue one helical turn upstream or downstream of the exact position of Asp[564] (see GPCR data base, GPCRdb, EMBL, Heidelberg). The functional importance of an anionic residue at the N-terminal end of TMD6 is further supported by mutagenesis studies with the M1 muscarinic acetylcholine receptor demonstrating that, like in the TSHR and LHR, the replacement of the corresponding Glu[360] with Ala results in a constitutively active receptor (62).

Next, we utilized direct structural information from the three-dimensional structure protein data base Protein Data Bank by searching for sequence motifs similar to a sequence fragment of the i3 loop/TMD6 junction of the LHR (DTKIA, amino acid positions 564–568). FASTA search revealed an almost identical sequence fragment (DTKAI) in the T7 DNA polymerase (Protein Data Bank code 1T7P; amino acid positions 235–239). Structural data from crystallographic studies with a resolution of 2.2 Å (63) indicate participation of Asp[235] in an N-terminal helix-capping conformation (Fig. 6A). The carboxyl moiety of the Asp[235] side chain forms a hydrogen bond toward the main chain NH group of Ala[238].

To visualize and evaluate the conformational consequences of a TMD6 helix capping for the intracellular portion of the LHR, a structural model was computed on the basis of a previously described TSHR model (12). The conformation of the i3 loop was assembled from overlapping sequence fragments found in the Protein Data Bank data base. The N cap structure found in the T7 DNA polymerase was used as a template to model the i3 loop/TMD6 junction of the LHR (Fig. 6B). The introduction of the helix-capping structure of TMD6 led to a remarkable difference compared with our former TSHR model.
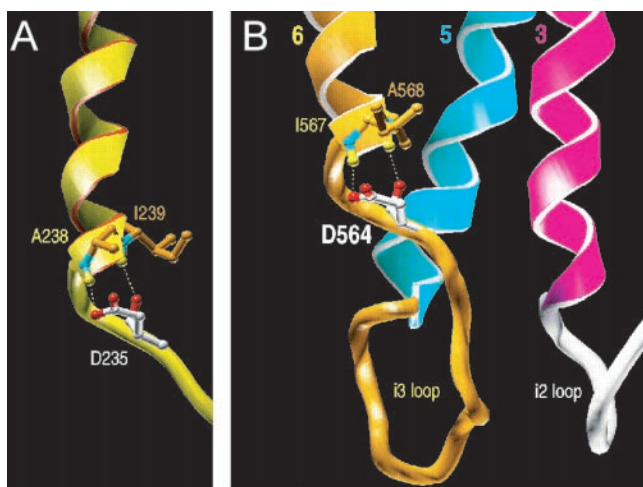
FIG. 6. **Proposed structure of an N cap motif at the N-terminal end of TMD6 of the LHR.** Mining the three-dimensional structure protein data base Protein Data Bank by searching for motifs similar to the sequence of the i3 loop/TMD6 junction of the LHR, we identified an almost identical sequence fragment (DTKAI) in the T7 DNA polymerase (Protein Data Bank code 1T7P; amino acid positions 235–239). Structural data from crystallographic studies indicate a participation of Asp[235] in an N-terminal helix-capping conformation (*A*). To terminate and stabilize the downstream helix the side chain carboxylate of Asp[235] (*red*) can form a hydrogen bond (*yellow dotted line*) with main chain NH group (*blue/yellow*) of Ala[238]. An additional hydrogen bond is established between the main chain oxygen of Asp[235] (*red*) and the NH group (*blue/yellow*) of the peptide backbone in position i+4. Based on a previously described TSHR model (12) and the NMR data of the peptide i3/TMD6, a model of the TMDs and the intracellular loops of the LHR was computed. The N cap structure found in the T7 DNA polymerase served as template to model the i3 loop/TMD6 junction of the LHR (*B*). In this model oxygen atoms of the backbone and side chain of Asp[564] interact with the NH backbone of residues Ile[567] and Ala[568] to form a helix-capping structure.

In particular, the participation of Asp[564], Ile[567], and Ala[568] in an N cap structure of TMD6 resulted in an orientation of these residues toward TMD3. In our model, this subsequent tight packing of the TMD3/i2 loop and the i3 loop/TMD6 junctions seals the inner TMD bundle. A similar effect is achieved by mutational extension (poly-Ala stretches) of TMD6 (not shown).

A large number of activating mutations have been identified for the glycoprotein hormone receptors with a majority clustered in TMD6 and the C-terminal part of the i3 loop. To condense the structural importance of all these vulnerable residues in one general mechanism of activation, it was suggested that single mutations perturb specific interhelical interactions between a tight hydrophobic packing between TMD5 and TMD6 as well as a specific H-bonding network in the center of TMD6 and TMD7 that stabilize the inactive receptor conformation (14). In addition to missense mutations, we have recently shown that large deletions (5–9 amino acids) within the i3 loop can position-independently activate the TSHR and the LHR (17, 19). What does the activation mechanism by a single amino acid substitution have in common with the receptor activation caused by large deletion mutations? Because the deletion of distinct amino acids residues did not account for the constitutive activity (19), it appears that the large deletion itself causes structural changes responsible for receptor activity. If this assumption holds true, reintroduction of arbitrary amino acids into the deletion should re-establish the inactive conformation of the receptor. To address this question the smallest deletion mutation of the LHR which caused a position-independent constitutive activity (LHR-Δ558–562) was used to introduce single Ala residues (Fig. 2*A*). As shown in Table II insertion of a single Ala in Δ558–562 (LHR-Δ558–562/1A) al-

ready restored normal basal receptor activity, and further Ala insertion (LHR-Δ558–562/2A) increased the E_{max} value to an extent comparable with those found with the wt LHR (Table II). This loop length-dependent receptor activation clearly suggests a mechanism in which a loop shortening dislocates or destabilizes the neighboring TMDs.

In summary, our new data in conjunction with recent studies attempting to clarify the mechanism of glycoprotein hormone receptor activation by mutations emphasize a scenario in which the inactive receptor conformation is stabilized not only by specific interhelical but also by intrahelical interactions. Because there is evidence of a direct participation of TMD6 in G-protein activation, it is reasonable to speculate that helix 6 is kept in a constrained inactive conformation by multiple intra- and interhelical forces. Disruption of one of these constraints relaxes the TMD6 structure and allows for an effective G-protein activation.

Note added in Proof—The recent crystal structure of rhodopsin that was published after the submission of this manuscript proposes that the residues of the conserved (D/E)RY motif participate in several hydrogen bonds with surrounding residues of TMD6 (65). However, the fine structure of this region was not finally resolved. Similar to our results, Glu[239] (Asp[564] in the LHR) is located at the very N-terminal end of TMD6. An interaction of Asp[564] with the Arg residue of the (D/E)RY motif, as suggested for the corresponding Glu[239] in rhodopsin, was excluded for the LHR by mutagenesis approaches (18, 19).

REFERENCES

1. Wess, J. (1998) *Pharmacol. Ther.* **80,** 231–264
2. Schertler, G. F., Villa, C., and Henderson, R. (1993) *Nature* **362,** 770–772
3. Unger, V. M., Hargrave, P. A., Baldwin, J. M., and Schertler, G. F. (1997) *Nature* **389,** 203–206
4. Yeagle, P. L., Alderfer, J. L., and Albert, A. D. (1995) *Nat. Struct. Biol.* **2,** 832–834
5. Yeagle, P. L., Alderfer, J. L., and Albert, A. D. (1995) *Biochemistry* **34,** 14621–14625
6. Yeagle, P. L., Alderfer, J. L., and Albert, A. D. (1997) *Biochemistry* **36,** 9649–9654
7. Yeagle, P. L., Alderfer, J. L., Salloum, A. C., Ali, L., and Albert, A. D. (1997) *Biochemistry* **36,** 3864–3869
8. Jung, H., Windhaber, R., Palm, D., and Schnackerz, K. D. (1995) *FEBS Lett.* **358,** 133–136
9. Jung, H., Windhaber, R., Palm, D., and Schnackerz, K. D. (1996) *Biochemistry* **35,** 6399–6405
10. Farahbakhsh, Z. T., Ridge, K. D., Khorana, H. G., and Hubbell, W. L. (1995) *Biochemistry* **34,** 8812–8819
11. Altenbach, C., Yang, K., Farrens, D. L., Farahbakhsh, Z. T., Khorana, H. G., and Hubbell, W. L. (1996) *Biochemistry* **35,** 12470–12478
12. Biebermann, H., Schöneberg, T., Schulz, A., Krause, G., Grüters, A., Schultz, G., and Gudermann, T. (1998) *FASEB J.* **12,** 1461–1471
13. Kjelsberg, M. A., Cotecchia, S., Ostrowski, J., Caron, M. G., and Lefkowitz, R. J. (1992) *J. Biol. Chem.* **267,** 1430–1433
14. Lin, Z., Shenker, A., and Pearlstein, R. (1997) *Protein Eng.* **10,** 501–510
15. Robinson, P. R., Cohen, G. B., Zhukovsky, E. A., and Oprian, D. D. (1992) *Neuron* **9,** 719–725
16. Porter, J. E., Hwa, J., and Perez, D. M. (1996) *J. Biol. Chem.* **271,** 28318–28323
17. Wonerow, P., Schöneberg, T., Schultz, G., Gudermann, T., and Paschke, R. (1998) *J. Biol. Chem.* **273,** 7900–7905
18. Kosugi, S., Mori, T., and Shenker, A. (1998) *Mol. Pharmacol.* **53,** 894–901
19. Schulz, A., Schöneberg, T., Paschke, R., Schultz, G., and Gudermann, T. (1999) *Mol. Endocrinol.* **13,** 181–190
20. Aurora, R., and Rose, G. D. (1998) *Protein Sci.* **7,** 21–38
21. Wan, W. Y., and Milner-White, E. J. (1999) *J. Mol. Biol.* **286,** 1633–1649
22. Marqusee, S., Robbins, V. H., and Baldwin, R. L. (1989) *Proc. Natl. Acad. Sci. U. S. A.* **86,** 5286–5290
23. Zhang, X. J., Baase, W. A., and Matthews, B. W. (1991) *Biochemistry* **30,** 2012–2017
24. Heinz, D. W., Baase, W. A., and Matthews, B. W. (1992) *Proc. Natl. Acad. Sci. U. S. A.* **89,** 3751–3755
25. Higuchi, R. (1989) in *PCR Technology* (Ehrlich, H. A., ed) pp. 61–70, Stockton Press, New York
26. Hitt, M., Bett, A. J., Addison, C. L., Prevec, L., and Graham, F. L. (1995) in *Viral Gene Techniques* (Adolph, K. W., ed) pp. 13–30, Academic Press, San Diego, CA
27. Salomon, Y., Londos, C., and Rodbell, M. (1974) *Anal. Biochem.* **58,** 541–548
28. Berridge, M. J. (1983) *Biochem. J.* **212,** 849–858

29. Gudermann, T., Birnbaumer, M., and Birnbaumer, L. (1992) *J. Biol. Chem.* **267,** 4479–4488
30. Henklein, P., Schubert, U., Kunert, O., Klabunde, S., Wray, V., Kloppel, K. D., Kiess, M., Portsmann, T., and Schomburg, D. (1993) *Pept. Res.* **6,** 79–87
31. Wüthrich, K. (1986) *NMR of Proteins and Nucleic Acids*, Wiley-Interscience, New York
32. Nilges, M., Clore, G. M., and Gronenborn, A. M. (1988) *FEBS Lett.* **239,** 129–136
33. Brünger, A. T. (1992) *X-PLOR, a System for X-ray Crystallography and NMR*, Yale University Press, New Haven, CT
34. Holm, L., and Sander, C. (1993) *J. Mol. Biol.* **233,** 123–138
35. Krause, G., Hermosilla, R., Oksche, A., Rutz, C., Rosenthal, W., and Schülein, R. (2000) *Mol. Pharmcol.* **57,** 232–242
36. Parma, J., Duprez, L., Van Sande, J., Cochaux, P., Gervy, C., Mockel, J., Dumont, J., and Vassart, G. (1993) *Nature* **365,** 649–651
37. Kosugi, S., Mori, T., and Shenker, A. (1996) *J. Biol. Chem.* **271,** 31813–31817
38. Chazenbalk, G. D., Nagayama, Y., Wadsworth, H., Russo, D., and Rapoport, B. (1991) *Mol. Endocrinol.* **5,** 1523–1526
39. Wang, H., Jaquette, J., Collison, K., and Segaloff, D. L. (1993) *Mol. Endocrinol.* **7,** 1437–1444
40. Zhu, X., Gudermann, T., Birnbaumer, M., and Birnbaumer, L. (1993) *J. Biol. Chem.* **268,** 1723–1728
41. Wang, Z., Hipkin, R. W., and Ascoli, M. (1996) *Mol. Endocrinol.* **10,** 748–759
42. Wallin, E., and von Heijne, G. (1995) *Protein Eng.* **8,** 693–698
43. Kyte, J., and Doolittle, R. F. (1982) *J. Mol. Biol.* **157,** 105–132
44. Serrano, L., and Fersht, A. R. (1989) *Nature* **342,** 296–299
45. Forood, B., Feliciano, E. J., and Nambiar, K. P. (1993) *Proc. Natl. Acad. Sci. U. S. A.* **90,** 838–842
46. Thapar, R., Nicholson, E. M., Rajagopal, P., Waygood, E. B., Scholtz, J. M., and Klevit, R. E. (1996) *Biochemistry* **35,** 11268–11277
47. Richardson, J. S., and Richardson, D. C. (1988) *Science* **240,** 1648–1652
48. El Masry, N. F., and Fersht, A. R. (1994) *Protein Eng.* **7,** 777–782
49. Boice, J. A., and Hightower, L. E. (1997) *J. Biol. Chem.* **272,** 24825–24831
50. Abell, A. N., and Segaloff, D. L. (1997) *J. Biol. Chem.* **272,** 14586–14591
51. Abell, A. N., McCormick, D. J., and Segaloff, D. L. (1998) *Mol. Endocrinol.* **12,** 1857–1869
52. Blondelle, S. E., Forood, B., Houghten, R. A., and Perez-Paya, E. (1997) *Biochemistry* **36,** 8393–8400
53. Greenfield, N., and Fasman, G. D. (1969) *Biochemistry* **8,** 4108–4116
54. Henry, G. D., and Sykes, B. D. (1994) *Methods Enzymol.* **239,** 515–535
55. Killian, J. A., Trouard, T. P., Greathouse, D. V., Chupin, V., and Lindblom, G. (1994) *FEBS Lett.* **348,** 161–165
56. Rigby, A. C., Grant, C. W., and Shaw, G. S. (1998) *Biochim. Biophys. Acta* **1371,** 241–253
57. Arshava, B., Liu, S.-F., Jiang, H., Breslav, M., Becker, J. M., and Naider, F. (1998) *Biopolymers* **46,** 343–357
58. Chopra, A., Yeagle, P. L., Alderfer, J. A., and Albert, A. D. (2000) *Biochim. Biophys. Acta* **1463,** 1–5
59. Soulie, S., Neumann, J. M., Berthomieu, C., Moller, J. V., le Maire, M., and Forge, V. (1999) *Biochemistry* **38,** 5813–5821
60. Wishart, D. S., Sykes, B. D., and Richards, F. M. (1992) *Biochemistry* **31,** 1647–1651
61. Hartmann, E., Rapoport, T. A., and Lodish, H. F. (1989) *Proc. Natl. Acad. Sci. U. S. A.* **86,** 5786–5790
62. Hogger, P., Shockley, M. S., Lameh, J., and Sadee, W. (1995) *J. Biol. Chem.* **270,** 7405–7410
63. Doublie, S., Tabor, S., Long, A. M., Richardson, C. C., and Ellenberger, T. (1998) *Nature* **391,** 251–258
64. Weiner, S. J., Kollman, P. A., Nguyen, D. T., and Case, D. A. (1986) *J. Comp. Chem.* **7,** 230–252
65. Palczewski, K., Kumasaka, T., Hori, T., Behnke, C. A., Motoshima, H., Fox, B. A., Le Trong, I., Teller, D. C., Okada, T., Stenkamp, R. E., Yamamoto, M., and Miyano, M. (2000) *Science* **289,** 739–745